Reliability of very low-grade metamorphic methods to decipher basin evolution: Case study from the Markstein basin (Southern Vosges, NE France)

Sébastien Potel, Tatiana Maison, Marine Maillet, Anta-Clarisse Sarr, Michael Patrick Doublier, Ghislain Trullenque, Rafael Ferreiro Mählmann

Applied Clay Science 134 (2016) 175–185

Contents lists available at ScienceDirect

Applied Clay Science

journal homepage: www.elsevier.com/locate/clay

Research paper

Reliability of very low-grade metamorphic methods to decipher basin evolution: Case study from the Markstein basin (Southern Vosges, NE France)

Sébastien Potel [a,*], Tatiana Maison [a], Marine Maillet [a], Anta-Clarisse Sarr [a], Michael Patrick Doublier [b,c], Ghislain Trullenque [a], Rafael Ferreiro Mählmann [d]

[a] B2R, Institut Polytechnique LaSalle Beauvais, Geosciences Department, 19 Rue Pierre Waguet, F-60026 Beauvais, France
[b] Geoscience Australia, Resources Division, Cnr Jerrabomberra Avenue and Hindmarsh Drive, Symonston 2609, ACT, Australia
[c] Centre for Exploration Targeting, School of Earth and Environment, University of Western Australia, 35 Stirling Highway, Crawley 6009, WA, Australia
[d] Technische Universität Darmstadt, Institut für Angewandte Geowissenschaften, Schnittspahnstraße 9, D-64287 Darmstadt, Germany

ARTICLE INFO

Article history:
Received 31 March 2016
Received in revised form 29 September 2016
Accepted 2 October 2016
Available online 18 October 2016

Keywords:
Clay minerals
Very low-grade metamorphic petrology
Chlorite geothermometry
Kübler Index
Basin evolution
Vosges

ABSTRACT

Low- and very low-grade metamorphic studies investigating the alteration and reaction progress of clay minerals are powerful tools to decipher the thermal evolution of sedimentary and inverted meta-sedimentary basins. Sheet silicates such as illite and chlorite are very common in sedimentary basin sequences. They can be used to determine the grade of diagenesis and low-temperature metamorphism as measured through the XRD: illite Kübler-Index (KI; illite "crystallinity" in older literature) and the chlorite Árkai-Index (ÁI; chlorite "crystallinity" in older literature), respectively. Although the ÁI method is considered to be slightly less sensitive than the KI method, a reliable correlation between both methods is often observed in metamorphic domains with a uniform heat-flow history and minor tectono-structural complexity. Complementary to these methods, the K-white mica *b* cell dimension provides a robust estimate of pressure facies reached in very low- to low-grade temperature domains.

Here, we present a case-study from the Markstein basin located in the Southern Vosges. The lithostratigraphic units in the basin are characterized by deep marine flysch sequences of Upper Devonian to Upper Visean age and volcano-clastic sediments, respectively. The Markstein basin is surrounded by granitoids with intrusion ages between 340 and 326 Ma. A previous study showed orogenic deformation characterized by regional folding, and a contact metamorphism found in an outer halo of the granitoids up to 1500 m away from the contact (delineated by the occurrence of biotite). Here we present a multi-disciplinary study combining mineral assemblages, illite and chlorite "crystallinity indices", and K-white mica *b* cell dimension. Our approach allows to (i) map in (great) detail the areal extent of both regional/burial metamorphic and contact metamorphic domains; (ii) reveal the metamorphic zonation within both domains; and (iii) better constrain regional/burial and contact metamorphic history. The contact metamorphic domain is characterized by the occurrence of biotite and/or actinolite and low K-white mica *b* cell dimensions, whereas the zone of incipient orogenic metamorphism yields KI and ÁI values of the high-grade diagenesis and anchizone with intermediate K-white *b* cell dimensions.

1. Introduction

The metamorphic grade of rocks which underwent "very low- and low-grade metamorphism" (as follows the term will include also grade of diagenesis) is difficult to assess. The classical methods applied are the so-called illite "crystallinity" and the vitrinite reflectance. The methods are dependent on several factors: while the dominant factor is duration of thermal metamorphism, they also depend on pressure and the kinetics in mineral and organic matter reaction progress, respectively. In metamorphic studies, contrary to the diagenesis research, the very low temperature range has been little considered due to few mineral-reaction isograds established (zeolites and phyllosilicates) and to diverse disequilibrium states in the rocks to be studied (Ferreiro Mählmann et al., 2012). For these reasons, most publications regarding the determination of grade of metamorphism deal with conditions above 300 °C and the first occurrence of neoformed metamorphic minerals with well-defined reaction-isograds such as biotite, chloritoid, and actinolite (Turner, 1968; Winkler, 1979; Bucher and Frey, 1994). Basic methods developed in low-temperature petrology

* Corresponding author.
E-mail address: sebastien.potel@lasalle-beauvais.fr (S. Potel).

http://dx.doi.org/10.1016/j.clay.2016.10.003
0169-1317/

of sedimentary rocks applied in very low-grade studies use clay mineral indices. In this field, changes in the shape and sharpness ratio of the XRD 10 Å illite peak are characteristic for changes in grade of incipient metamorphism. It is recognized that a steady increase in the height-to-width ration of the 10 Å peak occurs with increasing diagenetic/incipient metamorphic grade (Weaver, 1961). Since Kübler (1967), illite "crystallinity" (IC) is used as a parameter, empirically related with the aggradation of illite (Ferreiro Mählmann et al., 2012). Temperature is believed to be the most important parameter affecting the IC (Kübler, 1967, 1968). As a rule, the IC value decreases (i.e., "crystallinity" increases) with increasing temperature (i.e. during sedimentary burial or tectonic overburden). The change in the IC value is attributed to: 1) a decrease of the proportion of swelling mixed-layers (especially at low-temperature diagenetic conditions); 2) an increase of the mean thickness of crystallites, often caused by a decrease in the amount of defects affecting the coherency of layer-to-layer bonding; 3) a decrease of lattice strain of crystallites (Merriman and Peacor, 1999; Árkai et al., 2002). This is best illustrated in contact metamorphic aureoles and is also supported by a small number of hydrothermal experiments (Krumm, 1984). In addition, some crystal-chemical clay parameters, like the measurement of the K-white mica *b* cell dimension (Sassi, 1972; Sassi and Scolari, 1974) can be used to decipher the metamorphic evolution of the rocks. This method is used as an estimate of pressure facies reached in low-grade meta-pelitic rocks (Frey and Robinson, 1999). Recently, Potel et al. (2006) have shown that this method is less prone to resetting than KI and the K-white mica *b* cell dimension. In New Calediona it preserved early K-white mica neoformation conditions after a pluri-facies metamorphic evolution.

In summary, it is recommendable to use a multi-method clay-mineral approach for deciphering orogenic histories and in general geodynamic scenarios and -if possible- a combined investigation of mineralogical and organo-petrological methods (Ferreiro Mählmann et al., 2012). The aim of the present paper is to test the reliability of the different methods generally used to study metamorphic series implying clay minerals in a pluri-facies metamorphic evolution (burial and contact metamorphisms).

2. Geological setting

In the Vosges, two of the central European Variscan Zones can be distinguished (Kossmat, 1927): the Saxothuringian zone in the north and the Moldanubian zone in the central and southern part (Fig. 1), both separated by a major SW-NE trending steep dipping fault, the shear zone of Lalaye Lubine (LLSZ) (Edel and Fluck, 1989). The northern area represents the Saxothuringian part of the Vosges Mountains and consists of sedimentary and volcanic sequences of Precambrian (schists of Villé), Silurian (schists of Steige) and Devonian to Early Carboniferous age (Bruche valley and Bande-médiane occurrences), and a series of dioritic to granitic plutons of early Carboniferous age. The central and southern, Moldanubian parts consist of very low- to high-grade metamorphic sequences that were intruded by numerous granitoid plutons (intrusion ages between 340 ± 2 and 345 ± 2 Ma, Schaltegger et al., 1996). The variscan basement (peak metamorphism at 337 to 334 Ma, Schaltegger et al., 1999) is divided into an upper, high-grade unit (granulites with garnet peridotites, leptynites, kinzingites and amphibolite facies paragneiss) and an underlying medium grade unit with migmatic paragneiss and anatectic orthogneiss with granite neosomes (Kalt et al., 1994; Kalt and Altherr, 1996). The southernmost part of the area is occupied by two main sedimentary basin, the Visean volcano sedimentary Markstein basin in the north and the Permian Giromagny basin in its south (Fig. 1).

In the Markstein basin, three sedimentary units can be distinguished (Jung, 1928): a northern allochtonous Markstein unit, and the southern autochtonous Oderen and Thann units. The Markstein unit is separated from the southern units by a thrust containing ophiolitic nappe fragments - the Klippen Belt (Jung, 1928) - which represents discontinuous exposures of serpentinized harzburgite, ophicalcite, gabbro, gneiss and conglomerate (Fig. 2). The Klippen Belt is interpreted as exhumed relicts from deep parts of small, marginal back-arc basins developed during closure of a Palaeozoic subduction (Skrzypek et al., 2012). The Markstein unit is formed by an Early Carboniferous siliciclastic turbidite sequence of flysch-like rocks (up to 3500 m thick) consisting of interbedded pelites and greywackes (Gagny, 1962; Krecher, 2005; Krecher et al., 2007). The volcano-sedimentary rocks of the autochtonous units are of Lower to Upper Visean age. The base of the Oderen unit is characterized by a succession of carbonates (probably of Frasnian age) overlain by Fammenian sediments and Early Carboniferous pelites and greywackes (Skrzypek et al., 2012). The Lower to Middle Visean sediments are composed of inter-bedded pelites and distal fine grained turbidites together with an associated volcanism documented by spilites (Maas, 1988; Schneider, 1990; Hammel, 1996).

The Markstein unit is framed to the west, north and east by granitic plutons, and is also intruded by syn-genetic microgranitic dikes (Gagny, 1968; Schaltegger et al., 1996) related to the "granite des Crêtes" (Gagny, 1968). The Metzeral granite intrusion, bordering the northern part of the Markstein basin, is dated at 341 ± 1 Ma (Schaltegger et al., 1996). The contact between sediments and granitoids is either a tectonic one formed by brittle faults and/or contact metamorphism as characterized by a secondary growth of biotites and hornblendes (Petrini and Burg, 1998). According to these authors, the contact metamorphism can be recognized in an outer halo up to 1500 m away from the intrusion contacts (based on the occurrence of microscopic and mesoscopic determined biotite and cordierite at the contact).

The whole Markstein formation is affected by intense folding causing the formation of tight structures with fold axis striking N130 to N140 (Fig. 2). This fold axis orientation is in agreement with results by Petrini and Burg (1998). The folding produces in places an intense cleavage best developed in the more competent layers, as already noticed by these last authors. According to Petrini and Burg (1998), regional deformation should have occurred about 340 Ma ago, i.e. shortly after deposition.

3. Materials and methods

3.1. X-ray diffraction

In pelitic rocks diagnostic minerals and mineral assemblages of the very low-grade metamorphic zone are scarce and only found in rocks with a very specific geochemical composition. In these rocks, the transitions from non-metamorphic to low-grade (referring to the term greenschist facies of Winkler, 1979) and from the very low-grade (chlorite zone of Tilley, 1925) to low-grade metamorphic zone (biotite zone of Barrow, 1893) take place through the diagenetic zone, the anchizone and the epizone (according to Kisch, 1987), each zone being characterized by specific values of the illite Kübler Index (Kisch, 1987; Árkai et al., 2003, 2007). The illite "crystallinity" (IC) or Kübler-Index (referring to the pioneer study of Kübler, 1964) is defined as the full width at half maximum (FWHM) of the first illite basal reflection in XRD patterns and expressed in Δ°2θ (Frey, 1987; Guggenheim et al., 2002). Guggenheim et al. (2002) recommended that the use of the term "crystallinity index" should be avoided, although it may be placed within quotation marks when referring to previously referenced work. They also recommended to refer the values to an index by citing the author describing the procedures to generate the index value. The proposed way of citing is much more important because the IC method is not calibrated uniformly (Kisch et al., 2004). Therefore, we will refer for 10 Å FWHM values to the illite "crystallinity" for raw data and to KI after calibration against Kübler's scale (Table 2).

IC is considered to be a function of crystallite thickness, the number of lattice defects (Merriman et al., 1990) and the peak interference with discrete smectite or illite-smectite mixed layer composition (Ferreiro Mählmann et al., 2012). Temperature is thought to be the main factor

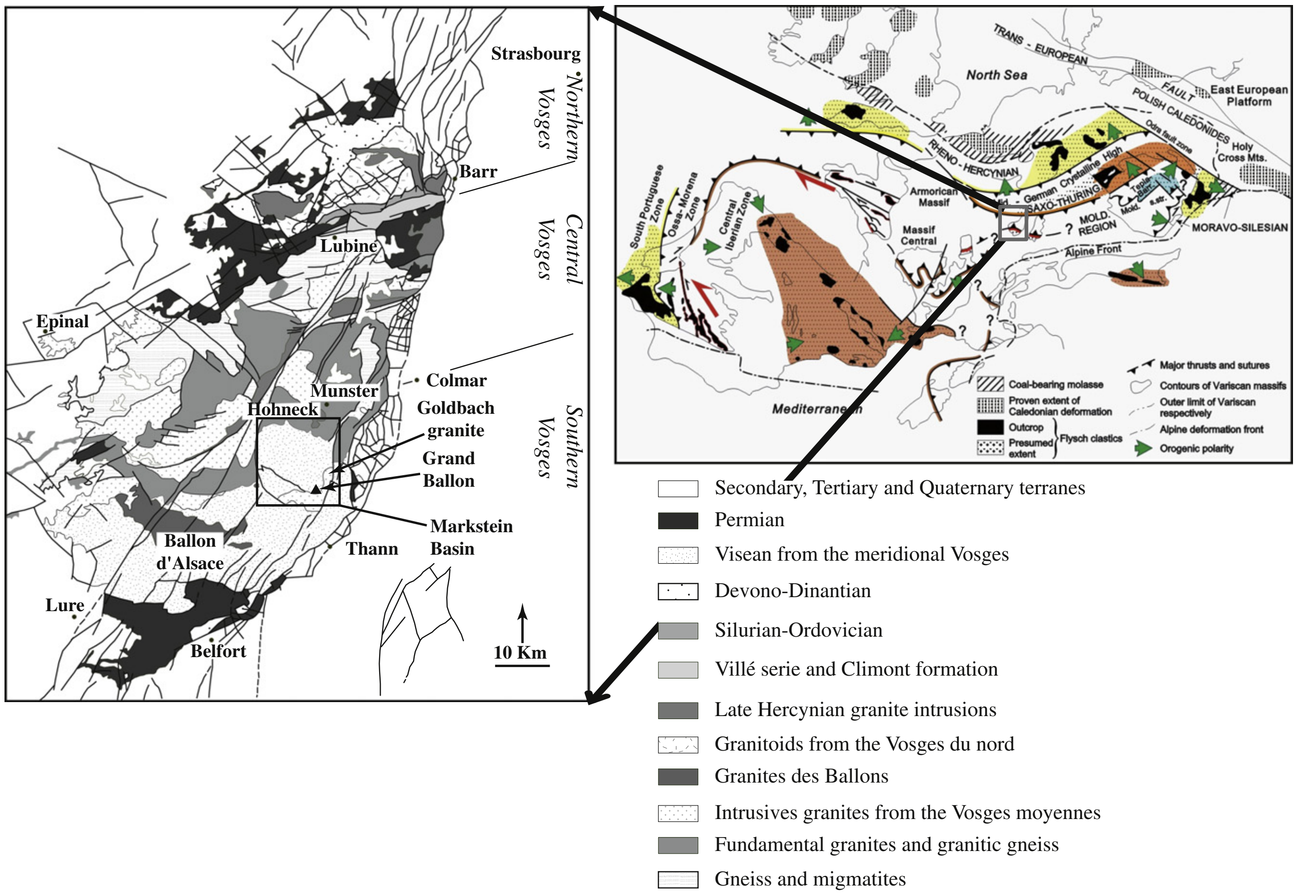

Fig. 1. Structural map of the Vosges showing the major tectonic units, after Tabaud et al. (2014). Onset showing the Variscan belt and the localization of the Vosges, modified after Franke (2000).

controlling the IC, but other parameters like lithology, time, tectonic stress and fluid/rock ratio may be important (see Frey, 1987; Árkai et al., 2002). For the evolution of chlorite during diagenesis and very low-grade metamorphism, Árkai (1991) and Árkai et al. (1995) proposed the chlorite "crystallinity" (ChC) or Árkai-Index (ÁI, according to Guggenheim et al., 2002) to monitor the reaction's progress.

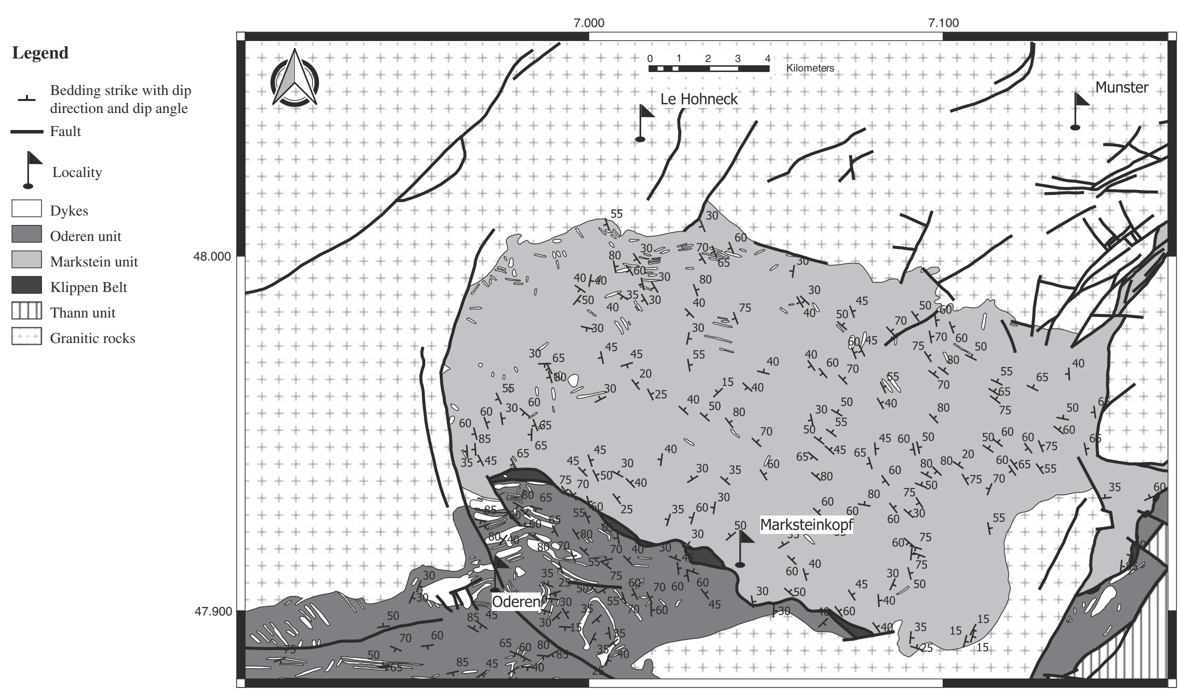

Fig. 2. Structural map of the Markstein basin showing bedding strike and dip angle. Lithological map of the Markstein basin modified after Skrzypek et al. (2012).

Mineral quantification in the samples was performed on whole-rock powder specimen, using the software DIFFRACPlus EVAL v 12.0 (©Bruker AXS). This method is based on the determination of the peak intensity in counts per second of the ten most representative peaks of the specific mineral.

The minerals quartz, feldspars, actinolite and sheet silicates are determined by thin section studies and X-ray diffraction analyses. Specifically for the sheet silicate determination, powder samples; air-dried, ethylene-glycolated and to 550 °C heated textured samples were used to precisely characterize the different micas as pyrophyllite, muscovite and biotite, but also the clay minerals.

3.1.1. Experimental conditions

X-ray diffraction analysis was performed using a D8-Advance Bruker-AXS (Siemens) diffractometer, Ni-filtered CuKα radiation at 40 kV and 40 mA and primary soller slit of 2.5° and divergence slit of 0.6 mm; secondary soller slit of 2.5°, with detector slit of 0.1 mm and antiscattering slit of 0.6 mm. Samples were crushed using an agate mortar pestle mill. Analyses of the relative content of minerals were performed with a step length of 0.02° and a scan speed of 1.2°/min over the range 2°–70°2θ for whole rocks composition.

For air-dried, ethylene glycol solvated and heated samples, measurements were performed with a step length of 0.02° and a scan speed of 0.6°/min over the range 2°–35°2θ.

3.1.2. Illite and chlorite indices

Seventy samples were collected in the Markstein basin (Table 1).

Clay mineral separation was conducted using techniques described by Schmidt et al. (1997) and following the recommendations of Kisch (1991). For the XRD analyses of ≤2 μm fractions, textured specimen were prepared and measured, air-dried, after solvation with ethylene glycol, and after heating (550 °C). These three analytical steps are routinely used to better determine clay minerals content and swelling properties. IC was calculated using the software DIFFRACPlus EVAL v 12.0 (©Bruker AXS). IC values were calibrated using the "crystallinity" index-standard (CIS) samples of Warr and Rice (1994) ($KI_{CIS} = 2.5734 * IC_{IPLB} - 0.1348$). The IC_{IPLB} represents the raw data FWHM as measured at the Institut Polytechnique LaSalle Beauvais (IPLB). The Kübler-Index is used to define the limits of metamorphic zones, following the recommendations for Kübler-Index calibration of Ferreiro Mählmann and Frey (2012) and the CIS-KI transformation formalism of Warr and Ferreiro Mählmann (2015). The zone boundary values were chosen as follows: KI = 0.25 Δ°2θ for the epizone to high anchizone boundary, KI = 0.33 Δ°2θ for the high to low anchizone boundary and KI = 0.42 Δ°2θ for the low anchizone to low diagenetic zone and KI = 1.00 Δ°2θ for the high diagenetic zone to low diagenetic zone (Table 1). The same experimental conditions were used to determine chlorite "crystallinity" on the 7 Å (002) peak of chlorite, where (ChC(002)) corresponds to the FWHM value of the second (7 Å) basal reflection. The ChC(002) measurements were also standardized with the CIS sample-set of Warr and Rice (1994) and expressed as the Árkai index (ÁI) according to the formulism proposed by Guggenheim et al. (2002): ÁI = 1.621 * ChC(002) + 0.006. The anchizone boundaries for the Árkai-Index were defined by correlation with the Kübler index at 0.30 Δ°2θ for the epizone to anchizone boundary and 0.35 Δ°2θ for the anchizone to diagenetic zone boundary.

Table 1
Metamorphic zone boundaries for Kübler Index (KI) and Árkai Index (ÁI) values after Warr and Ferreiro Mählmann (2015).

Metamorphic grade	KI	ÁI
Diagenesis	0. 42	0. 35
Lower Anchizone	0 . 3 3	
Upper Anchizone	0 . 25	0 . 30
Epizone		

3.1.3. Illite polytypism and K-white mica b cell dimension

K-white mica *b* cell dimension (or *b* cell dimension) was determined using samples free of mixed-layered minerals and biotite, and of anchizonal grade (Padan et al., 1982). The *b* cell dimension is based on the $d_{060,331}$ spacing and related to the increasing celadonite (Al-Si) substitution that occurs at given cation availability with pressure increase in white mica (Ernst, 1963; Guidotti et al., 1989). Guidotti et al. (1989) presented linear regression equations that quantify the changes in the *b* cell dimension of muscovite $2M_1$ that result from cation substitutions in the interlayer and octahedral sites. This *b* cell dimension value was determined by measuring the d position of the (060, 331) peak of the potassic white mica following the procedure of Sassi and Scolari (1974). The method allows characterizing the baric type of metamorphism. The metamorphic thermal gradients are inferred from the pressure facies series of metamorphism, as follows: K-white mica *b* cell dimensions <9.000 Å correspond to low-pressure facies series (metamorphic thermal gradient >35 °C/km); between 9.000 Å and 9.040 Å, a medium pressure facies series (metamorphic thermal gradient 25–35 °C/km); and larger than 9.040 Å for high-pressure facies series (metamorphic thermal gradient <25 °C/km). These thermal gradients correlate with hyperthermal, normal thermal and hypothermal gradients respectively determined by the correlation of KI values with vitrinite reflectance measurements (Ferreiro Mählmann et al., 2012).

Illite-muscovite polytype determination was performed using the $2M_1/(2M_1 + 1\,M)$ peak ratio equation. The peak intensities were calibrated with a series of synthetic illite polytypes mixtures following the technique described by Dalla Torre et al. (1994). Merriman and Peacor (1999) recognized that the wealth of data on variations in white mica polytypism as a function of temperature is generally consistent with predictable trends.

3.2. SEM-EDX

Chemical compositions of chlorites was analyzed and used for chlorite geo-thermometric determinations. The chemical phase composition was identified with an EDX-SEM (scanning electron microscope) operating a Hitachi S3400N SEM and equipped with a Thermo Ultradry EDX probe at the Institut Polytechnique LaSalle Beauvais. A NORAN-type correction procedure was used for all data reduction and all Fe was assumed to be ferrous for simplification. This is a strong simplification and may cause a limited use in chlorite thermometry if ferric Fe is present in chlorite (Inoue et al., 2009). An electron microprobe analysis (EMPA) would give a higher precision on the chemical composition and refine the temperature determination. Therefore here, chlorite geothermometry is shown as preliminary results and used as indicator.

Carbonated polished thin sections were analyzed using a 60 nA beam current, an accelerating voltage of 15 kV, an acquisition time of 30 s, and scanned over an area of 10 mm^2.

3.2.1. Chlorite geothermometer

The chlorite geothermometry was carried out following the geothermometers established by Inoue et al. (2009) and Bourdelle et al. (2013).

The Bourdelle et al. (2013) chlorite geo-thermometer accounts applicable for all low-T chlorite compositions (T < 350 °C; P < 4 kbar), but specifically for Si-rich compositions that characterizes diagenetic chlorites. To ensure the appropriate composition of chlorites the chlorite chemistry was determined with the EDX-SEM device. From these results, the cationic repartition in the structure is defined, assuming an ordered distribution on the crystal sites and thus determining the end-members ideal activities. The semi-empirical T = f(log K) geothermometer is formulated as a function of K, the equilibrium constant of the end-member-component reaction describing the chlorite + quartz equilibrium (function as activity).

$$T(^\circ C) = \frac{9400}{23.40 - \log x} - 273$$

$$\text{Where } x = \frac{\left(a^3_{Mg\text{-}Am}\right)}{\left(a_{Mg\text{-}ChlS}\right)\left(a^3_{Mg\text{-}Sud}\right)}$$

and Mg-Am: Mg-Amesite; Mg-ChlS: Mg-Chl semi-ordered; Mg-Sud: Mg-Sudoite.

The Inoue et al. (2009) geo-thermometer considers low-T disordered chlorites formed in diagenetic to very low-grade metamorphic environments. The four end-member components used are: Al-free trioctahedral chlorite (Afch), corundophilite (Crdp), chamosite (Chm) and sudoite (Sud), together with the assumption that octahedral cations and vacancies are randomly distributed in the *M* sites. The same EDX-SEM analyses as used for the Bourdelle et al. (2013) chlorite geo-thermometer were used. From these results, the cationic repartition in the sheet silicate structure is defined, based on the hypothesis of a steady Si and Al layer order in tetrahedral sites but a random mixing in a single type of octahedral site. Then the logarithmic ideal activity is determined. The geo-thermometer is formulated as:

$$T(^\circ C) = \frac{1}{0.00264 - 2.897 \times 10^{-4} x} - 273$$

$$\text{Where } x = \log K\prime = 3\log a^{ideal}_{crdp} - 3\log a^{ideal}_{sud} - \log a^{ideal}_{Afch}$$

3.3. Vitrinite reflectance

The chemical kinetics that governs maturation is thought to be strongly temperature dependent (e.g. Taylor et al., 1998; Polissar et al., 2011). It is known that although vitrinite reflectance is highly dependent on temperature (Le Bayon et al., 2011), optical properties of organic matter are also pressure dependent, as for vitrinite see e.g. Chandra (1965) or Dalla Torre et al. (1997). The recognition of characteristic optical changes was recently used to predict different pressure conditions (Ferreiro Mählmann and Le Bayon, 2016).

Vitrinite reflectance (VR) determinations were made on a Leitz microscope (Ortholux 2 POL BK) with a 125× oil-immersion objective (10× oculars) using monochromatic polarized light (546 nm) and a photomultiplier (MPV Leitz). In all cases, the R_{max} (mean value of maximum reflectance) and R_{min} (mean value of minimum reflectance) of vitrinite were determined. The photomultiplier was used to measure the reflectance intensity, which is determined through comparison with standards of known reflectance (Yttrium Aluminium Garnet single crystal, for the range of VR = 0.2 to 2.0%), Gallium Gadolinium Garnet single crystal (VR = 1.0 to 3.0%), Cubic Zirkonia (VR = 2.0 to 4.0%), Diamond (VR = 4.0 to 6.0%), Silicium Carbide (VR = 6.0 to >8.0%).

4. Results

The paragenesis found in the sedimentary samples from the Markstein (MAU) and Oderen (ODU) basins are presented in Tables 2 and 3, respectively. In the Markstein samples quartz, feldspars, chlorite and illite/muscovite are the predominant phases together with the metamorphic facies indicative minerals paragonite, actinolite and biotite occurring in variable quantities. In the Oderen samples, the same main phases are detected but without the occurrence of actinolite and paragonite.

4.1. Illite and chlorite indexes

The Kübler-Index (KI) and Árkai-Index (ÁI) were calculated from the FWHM of illite/muscovite and chlorite on the air-dry diffractogram respectively. The KI and ÁI values are given in Tables 2 and 3.

In the Markstein basin KI values range from 1.17Δ°2θ to 0.20Δ°2θ corresponding to metamorphic grades of the diagenetic zone to epizone, respectively. The larger values (i.e. lower metamorphic grades) are observed in the centre part of the unit, whereas at the basin border smaller values are measured. In contrast, in the Oderen basin, KI shows a narrower range of values between 0.72Δ°2θ and 0.48Δ°2θ, indicative of diagenetic zone metamorphic grade. Due to the interference on the 10 Å-peak, for samples containing biotite the KI was not determined. However, the occurrence of biotite implies epizone metamorphic conditions (Table 2). Biotite is one of the typical greenschist minerals traditionally used to distinguish the diagenesis from metamorphic conditions (Winkler, 1979), and recently used in meta-pelites to subdivide a lower greenschist facies (sub-greenschist) without biotite and greenschist facies with biotite. Because chlorite and feldspar are present in diagenetic rocks of the basins studied a reaction towards white mica + biotite + SiO_2 + H_2O is expected. Quartz aggregations and veins are very common in this metamorphic section of the basin showing that SiO_2 is in excess. At the western border of the Goldbach intrusion (Fig. 1), the white mica was determined by XRD as minor pyrophyllite and mainly muscovite, but chlorite is absent.

The relation between KI and ÁI is shown in Fig. 3. The correlation between the two "crystallinity" indices is only moderate ($R^2 = 0.39$), but a general trend shows a concomitant sharpening peak evolution of both with increasing grade of metamorphism.

The spatial distribution of samples and the metamorphic zones determined are shown in Fig. 4. An area of very low-grade metamorphism (diagenesis/lower anchizone) is located in the centre of the Markstein basin surrounded by an epizonal border area. In the central part of the very low-grade area a SW to NE increase in KI values is obvious, thus the sub-zones of high-grade diagenesis, low-grade anchizone and high-grade anchizone are oriented NW/SE. To the NE, the transition to the surrounding epizone is progressive. This is in contrast with the NW and SE part of the working area. Here, the transition to the epizonal domain along the border occurs over a much shorter distance and - to the south - samples of high diagenesis grade seem to directly abut the epizonal domain (Fig. 4). Biotite and actinolite are observed in samples from the epizone, and in all samples close to the plutons and the Klippen Belt (Fig. 4). Actinolite is restricted to samples closest to the magmatic rocks.

4.2. Illite polytypism and K-white mica b cell dimension

The percentages of the $2M_1$ polytype determined in different samples are shown in Fig. 4, varying between 32 and 100%. A close relationship between $\%2M_1$ and the KI can be observed. The complete conversion from $1M_d$ to $2M_1$ (% of $2M_1$ equal to 100) is reached at KI values of the high anchizone (Fig. 5).

The K-white mica *b* cell dimension (b_0 in Tables 2 and 3; Fig. 6) shows a spatial distribution, ranging between 8.938 and 9.027 Å, which is linked to KI results: high K-white mica *b* cell dimension values

Table 2
Paragenesis of studied samples in the Markstein Unit (MAU), FWHM (full width at half maximum intensity) of the (001) illite/muscovite reflection and (002) chlorite reflection and their values after calibration in KI and ÁI, respectively. K-white mica *b* cell dimension and %2 M1 illite/muscovite polytypes is given for samples where it was possible to determined them. n.d., not determined. Minerals abbreviations are from Kretz (1983).

Sample	Paragenesis							Illite/muscovite		Chlorite		b_0	$\%2M_1$
	Qtz	Fsp	Chl	Ill/mus	Act	Bt	Pg	FWHM001	KI	FWHM002	AI		
MAU01	38%	21%	17%	23%				0.261	0.38	0.199	0.33	9.008	58
MAU02	42%	24%	14%	20%				0.456	0.69	0.259	0.43	9.025	78
MAU03	24%	23%	28%	25%				0.290	0.43	0.217	0.36		
MAU04	43%	18%	18%	22%				0.265	0.39	0.272	0.45		
MAU05	38%	26%	10%	26%				0.371	0.56	0.260	0.43	9.027	32
MAU06	27%	44%	3%	9%	10%	8%		0.305	n.d.	0.197	0.33		
MAU07	38%	21%	11%	18%		11%		0.343	n.d.	0.175	0.29		
MAU08	30%	30%	9%	26%		5%		0.365	n.d.	0.255	0.42	8.980	
MAU09	31%	19%	20%	26%		5%		0.372	n.d.	0.235	0.39		
MAU10	20%	22%	39%	19%				0.643	1.00	0.223	0.37		
MAU11	12%	28%	14%	17%	29%			0.162	0.22	0.251	0.41		
MAU12	27%	14%	35%	23%				0.212	0.30	0.163	0.27		
MAU13	41%	19%	15%	24%				0.237	0.34	0.192	0.32	8.990	50
MAU14	29%	23%	26%	22%				0.221	0.31	0.179	0.30	9.007	55
MAU15	47%	19%	15%	20%				0.164	0.22	0.227	0.37	8.967	100
MAU16	32%	19%	21%	24%		4%		0.173	n.d.	0.141	0.23		
MAU17	32%	23%	14%	20%		11%		0.279	n.d.	0.178	0.29		
MAU18	25%	21%	28%	26%				0.209	0.30	0.203	0.33	9.009	100
MAU20	35%	33%	5%	17%		10%		0.316	n.d.	0.181	0.30		
MAU21	37%	20%	21%	22%				0.171	0.23	0.155	0.26	9.004	91
MAU22	34%	18%	24%	24%				0.281	0.47	0.216	0.36	9.010	54
MAU23	32%	17%	23%	23%		5%		0.460	n.d.	0.282	0.46		
MAU24	29%	17%	33%	21%				0.217	0.33	0.175	0.29	9.001	100
MAU25	45%	16%	6%	16%		17%		0.347	n.d.	0.234	0.39		
MAU26	19%	14%	51%	13%		3%		0.377	n.d.	0.180	0.30		
MAU27	26%	17%	22%	17%		19%		0.325	n.d.	0.225	0.37		
MAU28	28%	31%	17%	20%		4%		0.459	n.d.	0.181	0.30	9.000	
MAU29	36%	22%	14%	22%		5%		0.317	n.d.	0.226	0.37		
MAU30	39%	20%	16%	26%				0.594	1.17	0.265	0.44		
MAU31	10%	31%	9%	31%	11%	8%		0.285	n.d.	0.215	0.35		
MAU32	26%	24%	6%	18%		27%		0.274	n.d.	0.251	0.41		
MAU33	25%	24%	15%	19%		6%	11%	0.420	n.d.	0.209	0.34		
MAU34	9%	41%	11%	23%	12%	5%		0.278	n.d.	0.232	0.38		
MAU35	20%	45%	12%	23%				0.214	0.32	0.177	0.29		
MAU36	29%	24%	26%	21%				0.182	0.25	0.138	0.23		
MAU37	33%	25%	19%	23%				0.194	0.28	0.144	0.24		
MAU38	42%	30%	12%	16%				0.458	0.87	0.190	0.31		
MAU39	44%	21%	5%	21%		9%		0.291	n.d.	0.181	0.30		
MAU40	40%	20%	16%	19%		5%		0.288	n.d.	0.274	0.45		
MAU41	39%	20%	12%	29%				0.164	0.21	0.162	0.27		
MAU42	35%	16%	21%	27%				0.159	0.20	0.183	0.30		
MAU43	39%	22%	5%	29%		5%		0.220	n.d.	0.260	0.43		
MAU44	34%	21%	25%	16%		5%		0.453	n.d.	0.211	0.35		
MAU45	48%	10%	4%	14%	15%	9%		0.219	n.d.	0.131	0.22		
MAU46	35%	21%	20%	25%				0.211	0.32	0.148	0.25		
MAU47	40%	28%	4%	28%				0.279	0.47	0.259	0.43		
MAU48	37%	20%	15%	28%				0.215	0.32	0.215	0.35	8.938	88
MAU49	54%	13%	17%	14%		2%		0.275	n.d.	0.196	0.32		
MAU50	39%	20%	9%	18%		15%		0.348	n.d.	0.220	0.36		
MAU51	26%	36%	15%	23%				0.244	0.39	0.227	0.37		
MAU52	33%	22%	16%	24%		5%		0.243	n.d.	0.218	0.36		
MAU53	48%	9%	5%	38%				0.171	0.23	0.314	0.51		
MAU54	45%	16%	15%	24%				0.184	0.26	0.182	0.30		
MAU56	33%	23%	15%	28%				0.354	0.64	0.250	0.41	8.999	39

are located in the core of the basin, where high values of KI are observed. Low *b* cell dimension values are located at the periphery of the basin, in the biotite zone with low values of KI.

4.3. Chlorite geothermometer

Chlorite abundance in the analyzed samples for geo-thermometry is very irregular and ranges between 3 and 51% of the rock. The lowest chlorite contents are observed in the vicinity of the intrusions concomitant with an increase of the Illite/muscovite + biotite amount. Chemical analyses of chlorite are given in Table 4. Chlorite chemistry was normalised to 28 oxygens and fulfil the criterion $\Sigma Ca + Na + K < 0.2$ (Schmidt et al., 1997) used to test whether analyses are not contaminated by other phases. The analyzed chlorites have Mg/(Mg + Fe) ratios around 0.50 and Si contents below 3.00 a.p.f.u. (around 2.90 in average).

The temperatures determined with the chlorite geo-thermometer from Inoue et al. (2009) are presented in Fig. 6 and Table 4. In comparison, temperatures calculated with the Inoue et al. (2009) geothermometer are 100 to 150 °C higher than those calculated with Bourdelle et al. (2013), except for sample MAU46. Temperatures in the northern part of the Markstein basin are higher than those in the south (Oderen unit). The lowest T°C determined with chlorite thermometry (sample MAU 46) comes from the basin centre.

Table 3
Paragenesis of studied samples in the Oderen Unit (ODU), FWHM (full width at half maximum intensity) of the (001) illite/muscovite reflection and (002) chlorite reflection and their values after calibration in KI and ÁI, respectively. K-white mica *b* cell dimension and %2 M_1 illite/muscovite polytypes is given for samples where it was possible to determined them. n.d., not determined. Minerals abbreviations are from Kretz (1983).

Sample	Paragenesis							Illite/muscovite		Chlorite		b_0	%2M_1
	Qtz	Fsp	Chl	Ill/Mus	Act	Bt	Pg	FWHM001	KI	FWHM002	AI		
ODU01	25%	38%	11%	21%		4%		0.230	n.d.	0.209	0.34		
ODU02	40%	27%	14%	19%				0.390	0.72	0.230	0.38		
ODU03	23%	37%	10%	23%		7%		0.339	n.d.	0.220	0.36	9.020*	
ODU04	39%	28%	16%	16%				0.284	0.48	0.198	0.33		
ODU05	37%	35%	6%	18%		4%		0.360	n.d.	0.191	0.32		
ODU06	29%	43%	3%	20%		4%		0.302	n.d.	0.221	0.36		
ODU07	34%	27%	7%	26%		7%		0.404	n.d.	0.463	0.76		
ODU08	35%	29%	12%	20%		5%		0.348	n.d.	0.202	0.33		
ODU09	43%	15%	16%	21%		5%		0.335	n.d.	0.199	0.33		
ODU10	29%	29%	4%	29%		9%		0.357	n.d.				
ODU11	39%	24%	12%	16%			10%	0.301	n.d.	0.239	0.39		
ODU12	37%	25%	14%	18%		7%		0.246	n.d.	0.189	0.31		
ODU13	52%	16%	3%	16%		13%		0.305	n.d.	0.240	0.39		
ODU14	41%	20%	3%	21%		14%		0.275	n.d.	0.152	0.25		

4.4. Vitrinite reflectance

The vitrinite reflectance data obtained for sample ODU15 (from the Oderen unit) are given in Table 5. A second sample RFMV2000 is from the western border of the Goldbach intrusion (Fig. 1). Different geothermometers exist in the literature to relate vitrinite reflectance and paleo-temperatures. Barker and Pawlewicz (1986) first proposed a relationship for "normal" burial conditions between VR and the maximum temperature recorded by vitrinite coalification. Other geothermometers based on fluid inclusion calibrations in hydrothermal settings were also established and used here for comparison (e.g. Barker and Goldstein, 1990; Barker and Pawlewicz, 1994). The latter one is for hydrothermal conditions or rapid heating. These thermometric linear equations are time and pressure independent. It is known that VR is basically temperature dependent and time and pressure play a minor rule, depending strongly a the tectonic setting and the thermal gradient (see Le Bayon et al., 2011; Ferreiro Mählmann et al., 2012; Hartkopf-Fröder et al., 2015).

The VR obtained in the Oderen unit, show a mean R_{max} value of 6.9% and that of the Markstein unit a mean R_{max} value of 7.6%. It is important to stress that the original calibrations of all models used do not include high VR of the meta-anthracite and semi-graphite stage. Both measurements show a low bireflectance ($R_{min}\% = 2.9$ and 3.15% respectively). Due to the low bireflectance, the factor of strain and graphitization influenced vitrinite reflectance can be neglected (Ferreiro Mählmann and Le Bayon, 2016).

The temperatures calculated using the different geothermometers from Barker and Pawlewicz (1986) and Barker and Goldstein (1990) are around 400 °C. Lower temperatures are estimated using the equation of Barker and Pawlewicz (1994) with values of 286 and 291 °C, respectively. Barker and Pawlewicz (1986) pointed out that their equation calculates on the maximum paleogeotherm during maturation.

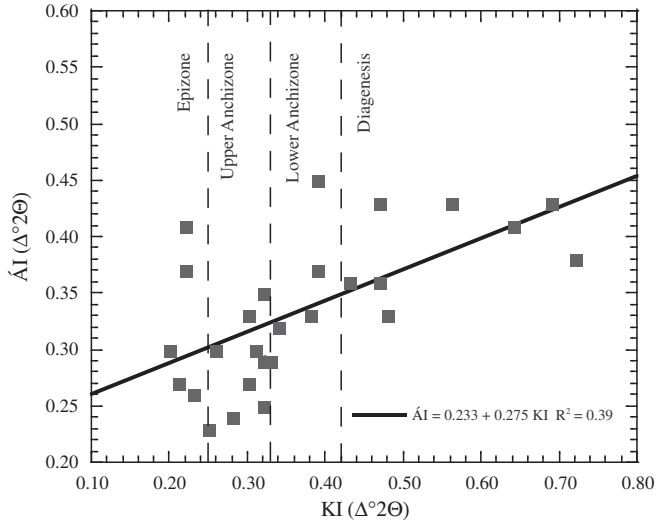

Fig. 3. Correlation between KI (10 Å) and ÁI (7 Å) values. Metamorphic zone boundaries are after Warr and Ferreiro Mählmann (2015).

5. Discussion

For both, the Markstein and the Oderen units, there is an apparent relation between sample location in the basin realm and metamorphic grade. Sub-greenschist to greenschist facies metamorphic grades are found at the basin border areas closely related to the surrounding granitic rocks, while in the basin centre diagenetic grade prevails.

The index mineral biotite associated with muscovite and actinolite but also paragonite and pyrophyllite are distributed at the outer parts of the basin and close to the granites. In contrast, no index minerals are observed in the centre of the basin (Fig. 4). This observation complements the findings of Petrini and Burg (1998), which described biotite occurrence up to 1500 m away from the granitic intrusion. Here, using XRD diffraction, it is possible to identify biotite in samples up to 3 km away from the contact due to the ability of the XRD to detect finer grained amounts. Because cordierite (Petrini and Burg, 1998) and pyrophyllite were observed at the intimate contact to the pluton and in granoblastic meta-sediments of hornfels character the contact metamorphic formation is best explained by metasomatism. The actinolite formation is very likely educt dependent and may relate to a former carbonate contend in the sedimentary rock. The reaction chlorite + feldspar = white mica + black mica + SiO_2 + H_2O is indicating temperatures at low pressures of 400 °C, but if buffered with a Fe authigenic phase also lower temperatures of 350 °C for neoformation is known (Brown, 1971; Bucher and Frey, 1994; Ferreiro Mählmann, 1996; Frey et al., 1999).

The main structure in the Markstein basin shows, in Fig. 2, predominantly N130-N140 strike with changing dip direction indicating an extensive folding at kilometre scale. The main deformation pattern was described in detail by Petrini and Burg (1998). At a more local scale, close to the intrusion and dykes, strike and dip are strongly disturbed. In this case, frequently the main foliation is missing. In the inner part of the basin, the mineral paragenesis detected is essentially composed of sheet silicates, which define the main schistosity. To the border of the basin, in some cases a biotite blastesis crosscuts the main schistosity.

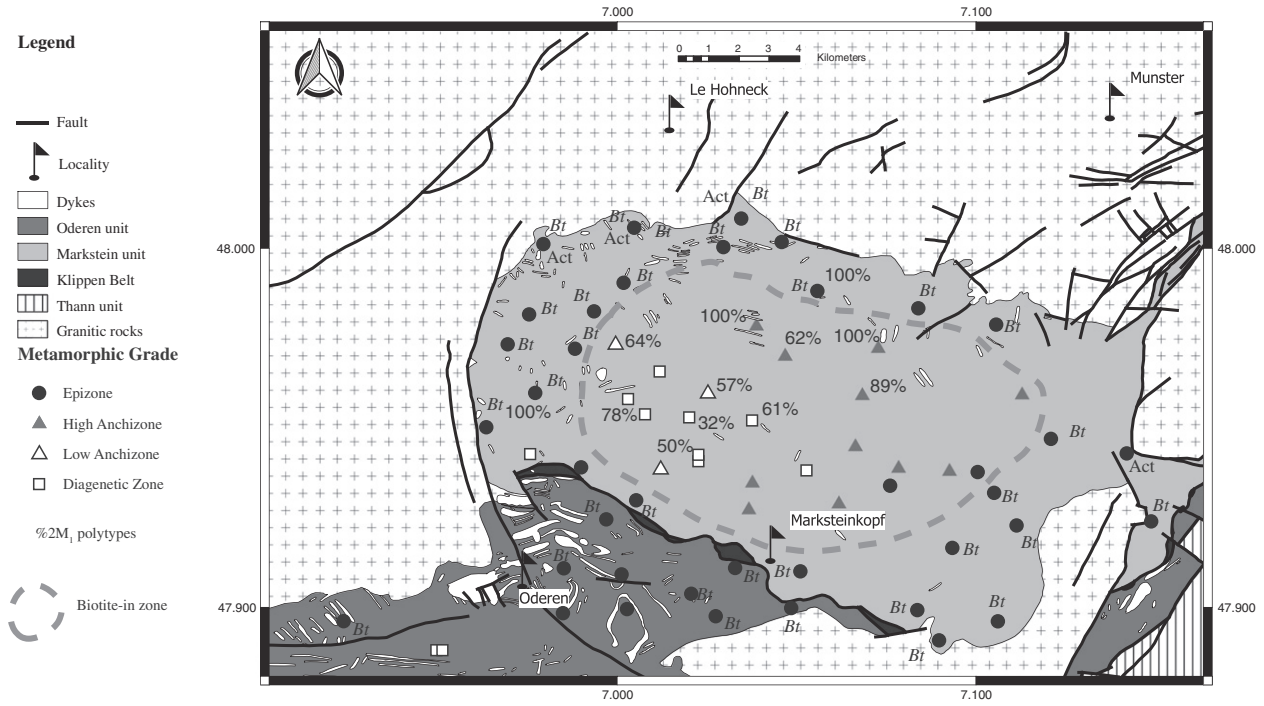

Fig. 4. Distribution of Kübler Index (KI) values, % $2M_1$ polytypes and minerals index (Bt: biotite; Act: actinolite) in the study area. Lithological map of the Markstein basin modified after Skrzypek et al. (2012).

According to Petrini and Burg (1998), the main schistosity is related to orogenic shortening. Thus, the blastesis is interpreted to be formed during the contact metamorphism.

The KI values display a similar trend to the mineral paragenesis in the Markstein basin, where the epizone is located at the outer parts of the basin showing increasing values to the centre of the basin with diagenetic conditions occurring north of Markstein (Fig. 4). In the Oderen unit, the KI values of samples with or without biotite indicate epizonal conditions between the Klippen Belt and the town Oderen (northern part of the Oderen unit, Fig. 4). More precision on the trends shown by KI and index minerals can be archived via integration with the %$2M_1$ polytypes. Like in New Caledonia, the complete conversion of from $1M_d$ to $2M_1$ is reached in the high anchizone (Potel et al., 2006) close to the epizone boundary (Brauckmann, 1984; Frey, 1987).

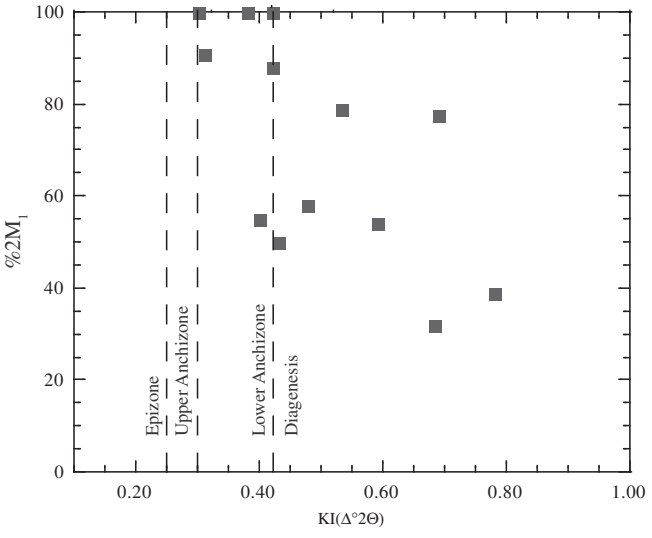

Fig. 5. Distribution pattern of %$2M_1$ K-white mica content of samples in the Markstein basin function of KI values.

Maxwell and Hower (1967) have shown that the complete conversion coincides or is close to the biotite isograd. The $2M_1$ values range between 32% at the north of Markstein (core of the basin) and 100% towards the border of the basin (Fig. 4).

Integration of the different parameters applied to estimate metamorphic grades demonstrates that the diagenetic to metamorphic trends along a basin transverse are well established. However, maximum temperature estimates from the different methods differ considerably: the results from Bourdelle et al. (2013) (Table 4) indicate the lowest mean temperatures between 169 and 230 °C. These temperatures are typical for the high-grade diagenetic zone (Frey and Ferreiro Mählmann, 1999). The clay mineral, organic matter and mineral metamorphic indicative relationships do not prove such diagenetic conditions. In comparison with all other parameters, the temperatures calculated with Bourdelle et al. (2013) appear to under-estimate peak thermal conditions. This could be due to the chlorite composition, which shows a Mg/(Mg + Fe) ratio of 0.50 whereas the geo-thermometer is calibrated on Fe-rich chlorite.

Higher temperatures in the same area (centre of the basin) are determined using the method of Inoue et al. (2009). In the range of error, including the simplification of referring Fe to be ferrous and that it is EDX analysis, the temperature estimation does not differ from the epizone of the Oderen unit (Fig. 2). The anchizone is mostly related to temperatures ranging between 230 ± 20 °C and 320 ± 30 °C in orogenic settings and most sedimentary basins and documented in generalized relationships with the same clay mineral indices used in the present study (Środoń, 1984; Weaver, 1989; Schiffman and Fridleifsson, 1991; Merriman and Frey, 1999). Referring to the same literature (e.g. Merriman and Frey, 1999; Potel et al., 2006), minimum temperature admitted for epizonal conditions is around 300 °C; thus temperatures calculated using the Inoue et al. (2009) geothermometer are still too low (mean 265 °C in the biotite free epizone). The temperature range estimated in the basin depot centre estimated between 230 and 300 °C are interpreted as burial and orogenic metamorphic peak temperature. These findings are in agreement with the K-white mica cell dimensions between 9.001 and 9.027 Å. In this area, the mineral neoformation, the illite aggradation and the mineral coarsening are related to the main

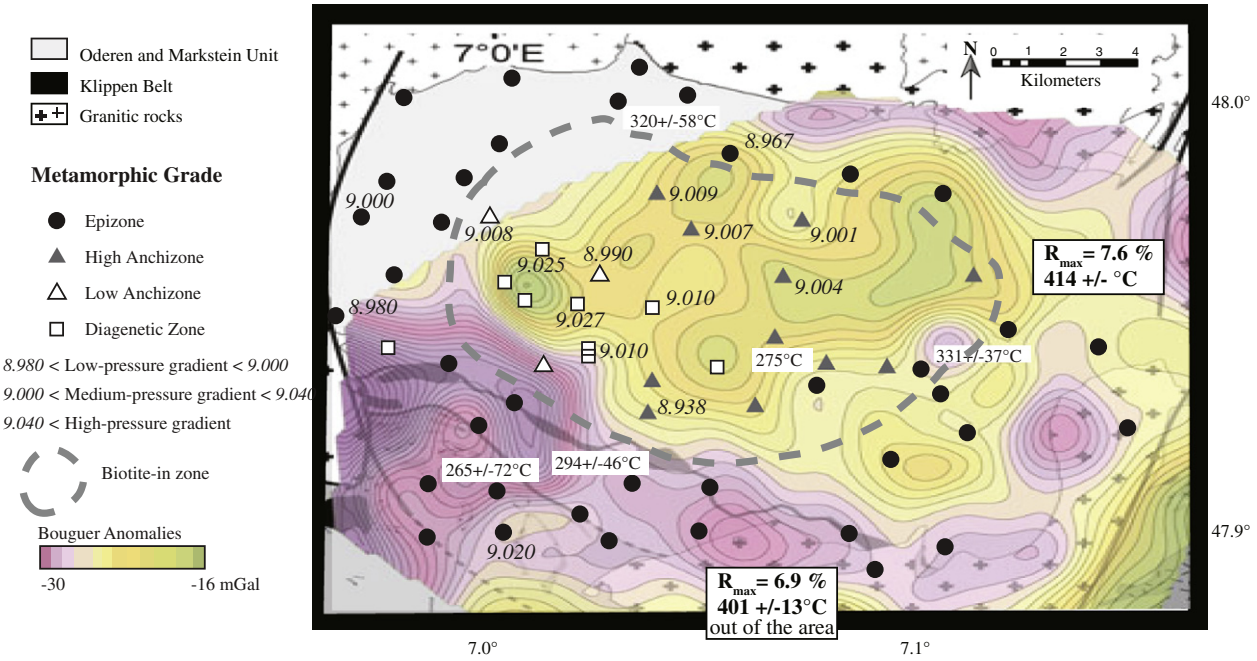

Fig. 6. Distribution of Kübler Index (KI) values, K-white micas *b* cell dimension. And temperatures calculated by chlorite chemistry based on geothermometer of Inoue et al. (2009) and by vitrinite reflectance thermometer based on the formulism of Barker and Pawlewicz (1994). The Bouguer anomaly map and the lithological map of the Markstein basin are redrawn after the map of Skrzypek et al. (2012).

foliation development during orogenic deformation and thus related to a barrovian metamorphism.

If the calculated values using Inoue et al. (2009) chlorite geothermometer from the biotite-zone boundary (Barrow, 1893) are compared with the possible existence of a biotite-in isograd (Winkler, 1979) also mean-temperature estimates of 294 to 331 °C are 20 to 100 °C too low. This contrasts with the mineral blastesis having a low biotite content, and indicating a low water activity (aH_2O). This means, that the reaction after Brown (1971) was formed between 350 and 400 °C.

These temperatures estimated from the biotite-isograd are consistent with the 401 to 414 °C calculated on the VR samples using the two geothermometers of Barker and Pawlewicz (1986) and Barker and Goldstein (1990) (Table 5). Nevertheless, it is to stress that in basin analysis, maturation is determined through basin modelling packages using the Sweeney and Burnham (1990) algorithm. Due to a restricted knowledge regarding the subsidence history, only partly recovered by the 3500 m thick sediment of the Markstein unit and unknown tectonic scenarios, these restrictions only allow to perform simple VR-°C conversion methods. Previous publications of Barker and Pawlewicz (1986, 1994) postulated equations for normal burial conditions and one for hydrothermal conditions and fast heating conditions, in our case evidenced by contact metamorphism. "One strength of this approach is the simple calculation of maximum paleotemperatures, one weakness is that just two heating rates are considered rather than a wide spectrum of heating rates in nature" (Hartkopf-Fröder et al., 2015). Nevertheless, a peak temperature >300 °C at the biotite-isograd and 400 °C at the contact to the pluton must be discussed according to the geodynamic setting, still to be proposed for the Markstein basin. According to the "simple thermal calculation" done by Petrini and Burg (1998), the temperature estimated at the sediments contact did not exceed 400 °C. On the other hand, using the temperature-pressure-time (T-P-t) equation of Dalla Torre et al. (1997) some information about the heating period is needed in order to judge if temperatures of 400 or up to 650 °C are in accordance with the thermal history in the inner halo of contact metamorphism. Regarding the K-white mica *b* cell dimension, a barrovian metamorphism is envisaged, followed by heating due to plutonism. In Dalla Torre et al. (1997), assuming a low pressure (<4 kbar) fit better using the formulism with a short heating time (<1 Ma) giving a calculated temperature around 400 °C.

Fig. 6 shows gravimetric results (Skrzypek et al., 2012) in relation with KI values, biotite occurrence and K-white mica *b* cell dimension. The low density zones seem to be related to granitic intrusions, which appear also to underlie the northernmost Oderen unit along the Klippen Belt. Higher densities are observed north of Markstein in the core of the basin, and have been related to increasing basin thickness (Skrzypek et al., 2012). This latter area corresponds also to high KI values (diagenetic zone to anchizone) with K-white mica *b* cell dimension values >9.000 Å

Table 4
Representative chemical analyses of chlorite based on 14 oxygens. Calculations are based on 14 oxygens (anhydrous basis). SD: standard deviation. Temperatures are calculated using the geothermometer from Inoue et al. (2009) and Bourdelle et al. (2013).

Sample N°	MAU26		MAU33		ODU09		ODU03		MAU46	
n	42	SD	24	SD	7	SD	3	SD	2	SD
Si	2.88	0.07	2.88	0.06	2.91	0.04	2.91	0.02	2.95	0.02
Ti	0.00	0.00	0.00	0.00	0.00	0.00	0.00	0.01	0.01	0.01
Al^{IV}	1.12	0.07	1.12	0.06	1.09	0.04	1.09	0.02	1.05	0.02
Al^{VI}	1.39	0.06	1.38	0.03	1.39	0.04	1.31	0.02	1.18	0.03
Fe^{2+}	2.24	0.12	2.29	0.09	2.24	0.11	2.35	0.03	2.35	0.21
Mn	0.01	0.02	0.01	0.02	0.01	0.03	0.04	0.01	0.00	0.00
Mg	2.22	0.13	2.19	0.12	2.21	0.05	2.16	0.07	2.35	0.18
Ca	0.01	0.01	0.01	0.01	0.00	0.00	0.01	0.01	0.00	0.00
Na	0.00	0.00	0.00	0.00	0.00	0.00	0.00	0.00	0.00	0.00
K	0.00	0.01	0.00	0.00	0.00	0.01	0.01	0.01	0.01	0.02
Mg/(Mg + Fe)	0.50	0.03	0.51	0.02	0.50	0.02	0.48	0.01	0.50	0.04
T°C Inoue	331	37	320	58	294	46	265	72	275	
T°C Bourdelle	187	29	171	10	169	20	189	03	230	13

Table 5
Vitrinite reflectance data for sample ODU15. Temperature are calculated from different geothermometers: (1) Barker and Pawlewicz (1986), (2) Barker and Goldstein (1990), (3) Barker and Pawlewicz (1994).

Sample	R_{max}	Std dev.	R_{min}	Std dev.	n.	T_1 (°C)	T_2 (°C)	T_3 (°C)
ODU15	6.9	0.7	2.9	0.7	30	401	393	286
RFMV2000	7.6	0.9	3.15	1.1	56	414	405	299

(up to 9.027 Å). Distribution of KI values indicate that epizonal conditions are closely related to zones of low density, and hence the distribution of granites. In these areas, the K-white *b* cell dimension values are close to or below 9.000 Å. The close relationship between clay mineral indices, Bouguer anomalies and intrusion contacts unequivocally demonstrate the thermal control of the epizone by magmatic heating.

The K-white mica *b* cell dimension values close to or below 9.000 Å are indicative of a low-pressure metamorphic facies (Sassi, 1972; Sassi and Scolari, 1974), which we interpret to be related to the contact metamorphism induced by the intrusion of the granitic rocks surrounding and partly underlying the basin. Assuming that a) the heating time at peak conditions was 5 Ma (time of the intrusion interval), and b) the pressure gradient was characteristic for a hyperthermal gradient, the T-P-t model of Dalla Torre et al. (1997) is re-considered. Therefore, a temperature of 600 to 650 °C at 1.0 to 4.0 kbar at the pluton contact is calculated (this is consistent with temperatures of 650 to 700 °C given for a granite melt at high aH_2O, Bucher and Frey, 1994). To explain cordierite in the inner halo at the hornfels pluton contact in the pelites to graywackes system, a temperature >530 °C is needed after Winkler (1974) and Winkler (1996). Assuming a higher Fe/Mg ratio as given in the Markstein basin, temperatures of 600 °C are reasonable (Bucher and Frey, 1994). Similar VR-T°C relationships were calibrated and modelled at the Vichuquén basin intrusions (Belmar et al., 2002) and at the Val Fredda Quartzdiorite (Ferreiro Mählmann et al., 2012). The KI-VR relationship found at the SW of the Golbach intrusion showing anchizone/epizone boundary KI-values and high meta-anthracite VR-values of 6.9 and 7.6 R_{max}% are plotted into the KI-VR thermal gradient diagram of Ferreiro Mählmann et al. (2012) indicative for hyperthermal heat flow conditions or contact metamorphism.

The higher values of K-white mica *b* cell dimension in the centre of the basin are better in accordance with a burial or orogenic metamorphism of medium pressure type. A VR study is missing in this part and a more detailed interpretation remains speculative.

6. Conclusion

The metamorphic evolution of the Markstein basin can be reconstructed with a multi-method approach involving metamorphic mineral assemblage formation, K-white mica evolution, vitrinite maturity and chemical analysis. The study allowed to decipher the range of different thermal events on the very low-grade to low-grade metamorphic pattern offering a powerful tool to reconstruct the thermal evolution of the basin. The K-white mica *b* cell dimension indicates the limit of the contact metamorphism effects to be more far reaching into the basin than shown by index minerals like biotite or actinolite. In this context it seems rather surprising that the Markstein basin centre, despite being surrounded by large plutons, still preserved burial or orogenic normal-thermal diagenetic to anchizone metamorphic rocks.

Comparing the methods to determine maximum temperatures it is likely that the chlorite-thermometers differ in their thermal significance. It also is to note that a microprobe analysis may give more accurate results. It must be demonstrated if the chlorite chemistry is appropriate to be applied for a particular thermometer. In case of the VR methods used much more data are needed and more information about the geodynamic evolution. In case of the Markstein basin it is difficult to fix the modelling parameters. Nevertheless, the thermometry used calibrated on burial and normal orogenic conditions most probably define much better the very low-grade and diagenetic zone temperatures. In case of the epizonal contact metamorphism the hydrothermal calibrated methodology is preferred. Also knowing that intrusion time lasted for 1 to 5 Ma using the VR-T-P-t model the upper range of temperature of >530 °C at the inner contact halo (hornfels), 400 °C at the sediment interface, >350 °C at the biotite zone boundary and >320 °C anchizone to epizone limit seems to be very realistic.

The study shows that also in small basins strongly dominated by pluton and dyke intrusions a pre-magmatic burial to orogenic thermal history can be restored by a multi-methodical very low-grade metamorphic study. A very important procedure to do so, is the application of indices to determine grade of metamorphism strongly dependent on very differing kinetics. The variations in the reaction progress of indices in respond to changing thermal conditions allows to recognize different steps of a temperature - pressure - time path and thus the time of mineralization. This can be also very important for exploration in hydrothermal, geothermal and hydrocarbon studies at a local scale.

Acknowledgements

We thank D. Chassagnac and M. Laffay for all the work done during their bachelor master on the field. We thank Prof. W. Franke for his support to this project. Rafael Ferreiro Mählmann likes to thank Prof. Rudolf Maass (Albert-Ludwigs-Univ. Freiburg, Germany) for the introduction in geology and meta-sedimentary rocks in the Vosges. The manuscript has benefited greatly from thoughtful revision from an anonymous reviewer, M. Cemal Göncüoğlu (Muddle East Technical University, Ankara) and the editor Emilio Galán.

References

Árkai, P., 1991. Chlorite crystallinity: an empirical approach and correlation with illite crystallinity, coal rank and mineral facies as exemplified by Palaeozoic and Mesozoic rocks of northeast Hungary. J. Metamorph. Geol. 9, 723–734.

Árkai, P., Sassi, F.P., Sassi, R., 1995. Simultaneous measurements of chlorite and illite crystallinity: a more reliable tool for monitoring low- to very low grade metamorphisms in metapelites. A case study from the Southern Alps (NE Italy). Eur. J. Mineral. 7, 1115–1128.

Árkai, P., Ferreiro Mählmann, R., Suchy, V., Balogh, K., Sýkorová, I., Frey, M., 2002. Possible effects of tectonic shear strain on phyllosilicates: a case study from the Kandersteg area, Helvetic domain, Central Alps, Switzerland. Schweiz. Mineral. Petrogr. Mitt. 82, 273–290.

Árkai, P., Faryad, S.W., Vidal, O., Balogh, K., 2003. Very low-grade metamorphism of sedimentary rocks of the Meliata unit, Western Carpathians, Slovakia: implications of phyllosilicate characteristics. Int. J. Earth Sci. 92, 68–85.

Árkai, P., Sassi, F.P., Desmons, J., 2007. Very low- to low-grade metamorphic rocks. In: Fettes, D., Desmons, J. (Eds.), Metamorphic Rocks: A Classification and Glossary of Terms: Recommendations of the International Union of Geological Sciences Subcommission on the Systematics of Metamorphic Rocks. Cambridge University Press, Cambridge, UK, pp. 36–42.

Barker, C.E., Goldstein, R.H., 1990. Fluid-inclusion technique for determining maximum temperature in calcite and its comparison to the vitrinite reflectance geothermometers. Geology 18, 1003–1006.

Barker, C.E., Pawlewicz, M.J., 1986. The correlation of vitrinite reflectance with maximum temperature in humic organic matter. Lect. Notes Earth Sci. 5, 79–81.

Barker, C.E., Pawlewicz, M.J., 1994. Calculation of vitrinite reflectance from thermal histories and peak temperatures. A comparison of methods. In: Mukhopadhyay, P.K., Dow, W.G. (Eds.), Vitrinite Reflectance as a Maturity Parameter: Applications and Limitations. ACS Symp Series vol. 570, pp. 216–229.

Barrow, G., 1893. On an intrusion of biotite-muscovite gneiss in the South-Eastern Highlands of Scotland and its accompanying metamorphism. Geol. Soc. London Quart 49, 330–358.

Belmar, M., Schmidt, S.T., Ferreiro Mählmann, R., Mullis, J., Stern, W.B., Frey, M., 2002. Diagenesis, low-grade and contact metamorphism in the Triassic-Jurassic of the Vichuquen-Tilicura and Hualace´n Gualleco basins, Coastal Range of Chile. In: Schmidt, S.T., Ferreiro Mählmann, R. (Eds.), Diagenesis and Low Grade Metamorphism vol. 82. Schweiz. Mineral. Petrogr. Mitt., pp. 375–392.

Bourdelle, F., Parra, T., Chopin, C., Beyssac, O., 2013. A new chlorite geothermometers for diagenetic to low-grade metamorphic conditions. Contrib. Mineral. Petrol. 165, 723–735.

Brauckmann, F.J., 1984. Hochdiagenese im Muschelkalk der massive von Bramsche und Vlotho. Bochum. Geol. Geotechn. Arb. 14, 1–195.

Brown, E.H., 1971. Phase relations of biotite and stilpnomelane in greenschsit facies. Contrib. Mineral. Petrol. 31, 275–299.

Bucher, K., Frey, M., 1994. Petrogenesis of Metamorphic Rocks. Springer-Verlag, Berlin; New York, p. c1994 (318 p).

Chandra, D., 1965. Reflectance of coals carbonized under pressure. Econ. Geol. 60, 621–629.

Dalla Torre, M., Stern, W.B., Frey, M., 1994. Determination of white K-mica polytype ratios: comparison of different XRD methods. Clay Miner. 29, 717–726.

Dalla Torre, M., Mählmann Ferreiro, R., Ernst, W.G., 1997. Experimental study on the pressure dependence of vitrinite maturation. Geochim. Cosmochim. Acta 61, 2921–2928.

Edel, J.B., Fluck, P., 1989. The upper Rhenish Shield basement (Vosges, Upper Rhinegraben and Schwarzwald): main structural features deduced from magnetic, gravimetric and geological data. Tectonophysics 169, 303–316.

Ernst, W.G., 1963. Significance of phengitic micas from low grade schists. Am. Mineral. 48, 1357–1373.

Ferreiro Mählmann, R., 1996. The pattern of diagenesis andmetamorphism by vitrinite reflectance and illite-cristallinity in Mittelbunden and in the Oberhalbstein. 2.

Correlation of coal petrography and of mineralogical parameters. Schweiz. Mineral. Petrogr. Mitt. 76, 23–46.
Ferreiro Mählmann, R., Le Bayon, R., 2016. Vitrinite and vitrinite like solid bitumen reflectance in thermal maturity studies: correlations from diagenesis to incipient metamorphism in different geodynamic settings. Int. J. Coal Geol. 157, 52–73. http://dx.doi.org/10.1016/j.coal.2015.12.008.
Ferreiro Mählmann, R., Frey, M., 2012. In: Bozkaya, Ö., Potel, S., Nieto, F. (Eds.), Standardisation, Calibration and Correlation of the Kübler-Index and the Vitrinite/Bituminite Reflectance: An Inter-laboratory and Field Related StudySwiss J. Geosci. 105, 153–170.
Ferreiro Mählmann, R., Botzkaya, O., Potel, S., Le Bayon, R., Šegvić, B., Nieto García, F., 2012. The pioneer work of Bernard Kübler and Martin Frey in very low-grade metamorphic terranes: paleo-geothermal potential of variation in Kübler-Index/organic matter reflectance correlations. A review. Swiss J. Geosci. 105, 121–152.
Franke, W., 2000. The mid-European segment of the variscides: tectonostratigraphic units, terrane boundaries and plate tectonic evolution. In: Franke, W., Haak, V., Oncken, O., Tanner, D. (Eds.), Orogenic Processes: Quantification and Modelling in the Variscan Belt Vol. 179. Geological Society Special Publications, London, pp. 35–62.
Frey, M., 1987. Low Temperature Metamorphism. Blackie, Glasgow and London.
Frey, M., Ferreiro Mählmann, R., 1999. Alpine metamorphism of the Central Alps. Schweiz. Mineral. Petrogr. Mitt. 79, 135–154.
Frey, M., Robinson, D., 1999. Low-Grade Metamorphism. Blackwell Science, Oxford.
Frey, M., Desmons, J., Neubauer, F., 1999. Alpine metamorphic map 1:500,000. Schweiz. Mineral. Petrogr. Mitt. 79, 1–4.
Gagny, C., 1962. Caractères sédimentologiques et pétrographiques des schistes et grauwackes du culm dans les Vosges méridionales. Bull. Serv. Carte Géol. Alsace Lorraine 15, 139–160.
Gagny, C., 1968. Pétrogenèse du granite des crêtes (Vosges méridionales, France). Mémoire, Nantes (546 p).
Guggenheim, S., Bain, D.C., Bergaya, F., Brigatti, M.F., Drits, V., Eberl, D.D., Formoso, M., Gala'n, E., Merriman, R.J., Peacor, D.R., Stanjek, H., Watanabe, T., 2002. Report of the AIPEA nomenclature committee for 2001: order, disorder and crystallinity in phyllosilicates and the use of the "crystallinity index". Clay Miner. 37, 389–393.
Guidotti, C.V., Sassi, F.P., Blencoe, J.G., 1989. Compositional controls on the a and b cell dimensions of $2M_1$ Muscovites. Eur. J. Mineral. 1, 71–84.
Hammel, C., 1996. Une faune nouvelle de trilobites (Brachymetopus, Namuropyge) dans le Viséen des Vosges du Sud. Conséquences stratigraphiques et paléoécologiques. Géobios 29, 745–755.
Hartkopf-Fröder, C., Königshof, P., Littke, R., Schwarzbauer, J., 2015. Optical thermal maturity parameters and orgnaic geochemical alteration at low grade diagenesis to anchimetamorphism: a review. Int. J. Coal Geol. http://dx.doi.org/10.1016/j.coal.2015.06.005.
Inoue, A., Meunier, A., Patrier-Mas, P., Rigault, C., Beaufort, D., Vieillard, P., 2009. Application of chemical geothermometry to low-temperature trioctahedral chlorites. Clay Clay Miner. 57, 371–382.
Jung, J., 1928. Contribution à la géologie des Vosges hercyniennes d'Alsace. Mémoire. Université de Strasbourg (480 p).
Kalt, A., Altherr, R., 1996. Metamorphic evolution of garnet-spinel peridotites from the Variscan Schwarzwald (Germany). Geol. Rundsch. 85, 211–224.
Kalt, A., Hanel, M., Schleicher, H., Kramm, U., 1994. Petrology and geochronology of eclogites from the Variscan Schwarzwald (F.R.G.). Contrib. Mineral. Petrol. 115, 287–302.
Kisch, H.J., 1987. Correlation between indicators of very low grade metamorphism. In: Frey, M. (Ed.), Low Temperature Metamorphism. Blackie, Glasgow & London, pp. 227–300.
Kisch, H.J., 1991. Illite crystallinity: recommendation on sample preparation, X-ray diffraction settings, and interlaboratory samples. J. Metamorph. Geol. 9, 665–670.
Kisch, H.J., Árkai, P., Brime, C., 2004. On the calibration of the illite Kübler index (illite "crystallinity"). Schweiz. Mineral. Petrogr. Mitt. 84, 323–331.
Kossmat, F., 1927. Gliederung der varistischen Gebirgsbaues. Abhandlungen des Sächsischen Geologischen Landesamts. vol. 1 pp. 1–39.
Krecher, M., 2005. Die Turbiditsandstein-Komplex der devono-karbonischen Markstein Gruppe im Oberelsass (NE-Frankreich) und ihre Beziehungen zu den moldanubischen Gesteinseinheiten von Schwarzwald und Vogesen. Dissertation zur Erlangung des Doktorgrades. Albert-Ludwigs-Universität Freiburg (308 p).
Krecher, M., Grimm, B., Müller-Sigmund, H., Behrmann, J.-H., 2007. Sedimentology and tectonic setting of Devonian-carboniferous turbidites and debris flow deposits in the Variscan Vosges Mountains (Markstein group, NE-France). Z. Dtsch. Geol. Ges. 158, 1063–1087.
Kretz, R., 1983. Symbols for rock-forming minerals. Am. Mineral. 68, 277–279.
Krumm, H., 1984. Anchimetamorphose im Anis und Ladin (Trias) der Nördlichen Kalkalpen zwischen Arlberg und Kaisergebirge-ihre Verbeitung und deren baugeschichtliche Bedeutung. Geol. Rundsch. 73, 223–257.
Kübler, B., 1964. Les argiles, indicateurs de métamorphisme. Rev. Inst. Fr. Petrole 19, 1093–1112.
Kübler, B., 1967. La cristallinité de l'illite et les zones tout à fait supérieures du métamorphisme. Etages tectoniques. Colloques Neuchâtel, pp. 105–122 18–21 Avril 1967.
Kübler, B., 1968. Evaluation quantitative du métamorphisme par la cristallinité de l'illite. Bull. Centre Rech. Pau, S.N.P.A. 2, 385–397.
Le Bayon, R., Brey, G.P., Ernst, W.G., Ferreiro Mählmann, R., 2011. Experimental kinetic study of organic matter maturation: time and pressure effects on vitrinite reflectance at 400 °C. Org. Geochem. 42, 340–355.
Maas, R., 1988. Die Südvogesen in variszischer Zeit. Neues Jb. Geol. Paläontol. Monat. 10, 611–638.
Maxwell, D.T., Hower, J., 1967. High-grade diagenesis and low-grade metamorphism of illite in the Precambrian Belt Series. Am. Mineral. 52, 843–856.
Merriman, R.J., Frey, M., 1999. Patterns of very low-grade metamorphism in metapelitic rocks. In: Frey, M., Robinson, D. (Eds.), Low-Grade Metamorphism. Blackwell Science, Oxford, pp. 61–107.
Merriman, R.J., Peacor, D.R., 1999. Very low-grade metapelites: mineralogy, microfabrics and measuring reaction progress. In: Frey, M., Robinson, D. (Eds.), Low-Grade Metamorphism. Blackwell Science, Oxford, pp. 10–60.
Merriman, R.J., Roberts, B., Peacor, D.R., 1990. A transmission electron microscope study of white mica crystallite size distribution in a mudstone to slate transitional sequence, North Wales, UK. Contrib. Mineral. Petrol. 106, 27–40.
Padan, A., Kisch, H.J., Shagam, R., 1982. Use of lattice paramater b0 of dioctahedral illite/muscovite for the characterization of P/T gradients of incipient metamorphism. Contrib. Mineral. Petrol. 79, 86–95.
Petrini, K., Burg, J.-P., 1998. Relationship between deformation, plutonism and regional metamorphism in the Markstein area (southern Vosges). Géol. Fr. 2, 13–23.
Polissar, P.J., Savage, H.M., Brodsky, E.E., 2011. Extractable organic material in fault zones as a tool to investigate frictional stress. Earth Planet. Sci. Lett. 311, 439–447.
Potel, S., Ferreiro Mählmann, R., Stern, W.B., Mullis, J., Frey, M., 2006. Very low-grade metamorphic evolution of pelitic rocks under high-pressure/low-temperature conditions, NW New Caledonia (SW Pacific). J. Petrol. 47, 991–1015.
Sassi, F.P., 1972. The tetrological and geological significance of the b_0 values of potassic white micas in low-grade metamorphic rocks. An application to the Eastern Alps. Tschermaks Mineral. Petrogr. Mitt. 18, 105–113.
Sassi, F.P., Scolari, A., 1974. The b_0 of the potassic white micas as a barometric indicator in low-grade metamorphism of pelitic schists. Contrib. Mineral. Petrol. 45, 143–152.
Schaltegger, U., Schneider, J.-L., Maurin, J.-C., Corfu, F., 1996. Precise U-Pb chronometry of 345–340 Ma old magmatism related to *syn*-convergence extension in the southern Vosges (Central Variscan Belt). Earth Planet. Sci. Lett. 144, 403–419.
Schaltegger, U., Fanning, C.M., Günther, D., Maurin, J.C., Schulmann, K., Gebauer, D., 1999. Growth, annealing and recrystallization of zircon and preservation of monazite in high-grade metamorphism: conventional and in-situ U-Pb isotope, cathodoluminescence and microchemical evidence. Contrib. Mineral. Petrol. 134 (2–3), 186–201.
Schiffman, P., Fridleifsson, G.O., 1991. The smectite-chlorite transition in drill-hole NJ-15, Nesjavellir geothermal field, Iceland: XRD, BSE and electron microprobe investigations. J. Metamorph. Geol. 9, 679–696.
Schmidt, D., Schmidt, S.Th., Mullis, J., Ferreiro Mählmann, R., Frey, M., 1997. Very low grade metamorphism of the Taveyanne formation of western Switzerland. Contrib. Mineral. Petrol. 129, 385–403.
Schneider, J.-L., 1990. Enregistrement de la Dynamique Varisque dans les Bassins Volcano-sédimentaires Dévono-dinantiens: Exemple des Vosges du Sud Thèse de doctorat: Université de Strasbourg (222 p).
Skrzypek, E., Tabaud, A.-S., Edel, J.-B., Schulmann, K., Cocherie, A., Guerrot, C., Rossi, P., 2012. The significance of Late Devonian ophiolites in the Variscan orogen: a record from the Vosges Klippen Belt. Int. J. Earth Sci. 101, 951–972.
Środoń, J., 1984. X-ray powder diffraction identification of illitic materials. Clay Clay Miner. 32, 337–349.
Sweeney, J.J., Burnham, A.K., 1990. Evaluation of a simple model of vitrinite reflectance based on chemical kinetics. Am. Assoc. Pet. Geol. Bull. 74, 1559–1570.
Tabaud, A.-S., Whitechurch, H., Rossi, P., Schulmann, K., Guerrot, C., Cocherie, A., Lardeaux, J.M., Janousek, V., Oggiano, G., 2014. Devonian–Permian magmatic pulses in the northern Vosges Mountains (NE France): result of continuous subduction of the Rhenohercynian Ocean and Avalonian passive margin. In: Schulmann, K., Martinez Catalan, J.R. (Eds.), The Variscan Orogeny: Extent, Timescale and the Formation of the European Crust. Geological Society, London http://dx.doi.org/10.1144/SP405.12 (Special Publications, 405. First published online April 1, 2014).
Taylor, G.H., Teichmüller, M., Davies, A., Diessel, C.F.K., Littke, R., Robert, P., 1998. Organic Petrology. Gebrüder Borntraeger, Berlin (704 pp).
Tilley, C.E., 1925. Metamorphic zones in the southern Highlands of Scotland. J. Geol. Soc. Lond. 81, 100–112.
Turner, F.J., 1968. Metamorphic Petrology: Mineralogical and Field Aspects. McGraw-Hill, New York.
Warr, L.N., Ferreiro Mählmann, R., 2015. Recommendations for Kübler Index standardization. Clay Miner. 50, 282–285.
Warr, L.N., Rice, A.H., 1994. Interlaboratory standardization and calibration of clay mineral crystallinity and crystallite size data. J. Metamorph. Geol. 12, 141–152.
Weaver, C.E., 1961. Clay Minerals of the Ouachita Structural Belt and adjacent foreland. 6120. Univ. Texas, Bur. Economics, Geology Publications, pp. 147–162.
Weaver, C.E., 1989. Clays, Muds and Shales. Developments in Sedimentology (vol. 44). Elsevier, Amsterdam.
Winkler, H.G.F., 1974. Petrogenesis of Metamorphic Rocks. (third ed.). Springer-Verlag, New York.
Winkler, H.G.F., 1979. Petrogenesis of Metamorphic Rocks. 5th ed. Springer, Berlin.
Winkler, B., 1996. The dynamics of H_2O in minerals. Phys. Chem. Miner. 23, 310–318.